



Phenobarbital inhibits osteoclast differentiation and function through NF- κ B and MAPKs signaling pathway

Wei Wang^{a,b,1}, Yuan Gao^{a,1}, Wenwen Zheng^b, Minqi Li^{a,*}, Xuexing Zheng^{b,*}

^a Department of Bone Metabolism, School of Stomatology, Shandong University, Shandong Provincial Key Laboratory of Oral Tissue Regeneration, Jinan, China

^b School of Public Health, Shandong University, Jinan, China

ARTICLE INFO

Keywords:

Phenobarbital
Osteoclast
NF- κ B pathway
MAPKs pathway
Bone loss

ABSTRACT

The purpose of this study was to determine the direct effects of phenobarbital (PB) on receptor activator of nuclear factor kappa-B ligand (RANKL) induced osteoclast differentiation and function in vitro and in vivo. Here, PB significantly inhibited osteoclast formation and bone resorption ability induced by RANKL in vitro. Meanwhile, intracellular signaling transduction analysis revealed PB specifically decreasing the phosphorylation level of nuclear factor kappa-light-chain-enhancer of activated B cells (NF- κ B) and mitogen-activated protein kinase (MAPK), respectively. Besides, oral administration of PB at the dose of 60 mg/kg/day for 6 weeks led to improve the bone loss and to decrease the activity on both osteoblast and osteoclast. This suppression effect is more obvious in osteoblast-induced bone formation than that on osteoclast-induced bone resorption. Taken together, our findings demonstrated that PB down-regulate osteoclast differentiation and activity through modulation of NF- κ B and MAPKs signaling pathway. The direct suppression effect on osteoclast can induce bone loss after long term oral administration. This bone loss is due to reducing bone turnover rate on both sides of bone formation and bone resorption.

1. Introduction

Regulated tightly by osteoblasts, osteoclasts are a kind of bone-resorbing multinucleated cells that differentiate from the monocyte macrophage lineage [1]. Macrophage-colony stimulating factor (M-CSF) [2] and RANKL [3,4] are two essential cytokines expressed by osteoblasts for the differentiation of osteoclasts. The first of the mentioned two is a constitutive consequence of osteoblasts expression, while the latter is one of the inducible productions responding to osteotropic hormones and factors such as 1 α ,25-dihydroxyvitamin D₃ [5]. M-CSF receptors and RANKL receptors (RANK) are expressed by osteoclast precursors, after which differentiate into osteoclasts in the presence of M-CSF and RANKL [3,5]. Nuclear factor of activated T cells c1 (NFATc1), which is a master transcription factor for osteoclast differentiation, is specifically and strongly induced from the RANKL-RANK interaction [6]. The dephosphorylated NFATc1, whose transcription itself is also induced by NFATc1 in osteoclast precursors [7], translocates into nuclei and leads to the transcription of targets such as cathepsin K (CK) and tartrate-resistant acid phosphatase (TRAP). Proven by recent research, a transcription factor named c-fos has played an important part in the differentiation of osteoclasts induced by NFATc1

[1,6]. Ruffled borders and sealing zones are formed by activated osteoclasts toward bone surfaces during bone resorption [8,9]. Cytoskeletal disrupting of osteoclasts sealing zones leads to the suppression of the activities of bone-resorbing by osteoclasts [10–12].

Epilepsy is defined by the presence of recurrent seizures. It is the most common neurological disorder affecting approximately 50 million people worldwide. Therapy with antiepileptic drugs (AEDs) achieves seizures control in approximately 70% of patients. However, the remaining 30% require lifelong treatment [13]. Meanwhile, it can be complicated by a wide variety of somatic comorbidities that impact the patient's overall quality of life.

PB, a sedative hypnotic barbiturate, is a kind of anticonvulsant drug that's widely used by World Health Organization in developing countries for treating seizures of epilepsy along with bipolar disorder, neuropathic pain, migraine prophylaxis and cancer, thanks to its economically low cost. Nevertheless, the use of this medicine has been reduced due to the occurrence of negative side effects including hypnosis, sedation, nystagmus, dizziness, excitement, ataxia, paradoxical hyperactivity, confusion, etc. [14–17].

Our study focuses on the problem of bone metabolism caused by AEDs application. It is well known that long-term administration of

* Corresponding authors at: School of Stomatology and School of Public Health, Shandong University, Wenhua West Road 44-1, Jinan 250012, China.
E-mail addresses: liminqi@sdu.edu.cn (M. Li), zhengxx2513@hotmail.com (X. Zheng).

¹ These two authors contributed equally to this paper.

AEDs can result in disorders of vitamin D, mineral, and bone metabolism. Hahn et al. reported that PB might diminish the plasma vitamin D₃ after its long-term application [18]. Jette et al. demonstrated that PB could increase the risks of fracture and bone loss [19]. Notably, Fitzpatrick et al. showed that PB had upregulated the activation of CYP450 which is responsible for the metabolism of vitamin D. After that, 25 (OH) vitamin D converts into inactive metabolites. The resulting decrease in 1,25 (OH)₂ vitamin D leads to reduced calcium absorption, with consecutive secondary hyperparathyroidism, increased bone resorption and accelerated bone loss [20]. Therefore, the bone loss induced by PB is thought to be mainly caused by a drug induced deficiency of vitamin D rather than direct effects of the treatment on bone.

However, the direct effects of PB on bone resorption are still unknown. In 2009, Koide et al. demonstrated that phenytoin has a direct suppressing effect on the differentiation and the function of osteoclasts through inhibiting NFATc1 expression [21]. We deduced that PB, as the same kind of drug, will exhibit specific results on osteoclast in vitro assays. Therefore, our study aims to find the direct effects of PB on osteoclast-induced bone resorption both in vivo and in vitro. We think that experiment will benefit the research of the mechanism of epilepsy patients' bone metabolism disorder after PB administration.

2. Materials and methods

2.1. Cells culture and antibodies

Murine RAW264.7 monocytic cell line was purchased from the Shanghai Cell Center (Shanghai, China). The Dulbecco's modified eagle medium (DMEM), penicillin/streptomycin, and fetal bovine serum (FBS) were from the Gibco-BRL (Gaithersburg, MD, USA). Recombinant soluble mouse RANKL were purchased from R&D Systems (Minneapolis, MN, USA). Specific antibodies against NF-κB p65, extracellular signal-regulated kinase (ERK), p38, c-Jun N-terminal kinase (JNK), phospho-NF-κB p65 (Ser536), phospho-ERK (Thr202/Tyr204), phospho-p38 (Thr180/Tyr182), phospho-JNK (Thr183/Tyr185), horseradish peroxidase-conjugated goat anti-rabbit and swine anti-rabbit were obtained from Cell Signaling Technology (Cambridge, MA, USA). Anti-NFATc1, anti-c-fos, anti-β-actin and anti-osteopontin (OPN) were from Abcam (Cambridge, MA, USA). Rabbit antibody against alkaline phosphatase (ALP) was generated by Oda et al. [22]. Phenobarbital was purchased from Solarbio (Beijing, China).

2.2. Osteoclast differentiation, TRAP staining and resorption pit formation assay

RAW264.7 cells were seeded in six-well plates and cultured in DMEM containing 10% FBS and 1% penicillin/streptomycin. 2 h later, they were treated with PB (during whole process of cell culture) at concentrations of at 0 μM, 20 μM, 100 μM, 200 μM and 400 μM, respectively. The cells were then stimulated with (20 ng/ml) RANKL for 7 days. The culture medium was changed to fresh medium every other day. After 7 days, TRAP staining was used to evaluate osteoclast differentiation. Cells were fixed with 4% paraformaldehyde for 5 min at room temperature and stained for TRAP staining which proceeded like our previous study [23]. Briefly, cells were submerged in a mixture of 3.0 mg of naphthol AS-BI phosphate, 18 mg of red violet LB salt, and 100 mL(+) tartaric acid (0.36 g) diluted in 30 ml of 0.1 M sodium acetate buffer (pH 5.0) for 15 min at 37 °C. Cell nucleus were counterstained with hematoxylin for 2 min. Multinucleated TRAP-positive cells with at least 3 nuclei were scored as osteoclast. Pit formation assay was performed using the Corning osteo assay surface multiple well plates (Corning, Inc., Corning, NY, USA). RAW264.7 cells were seeded in 96-well plates and cultured for 10 days performed like the one mentioned before. After that, plates were stained with Von Kossa to increase the contrast between pits and surface coating and observed under a light microscope. The percentage of the resorbed areas and the number of

resorption pits in three random resorption sites were measured under microscopic examination using Image Pro Plus 6.2 software. The assays were performed in triplicate, and a representative view from each assay was presented.

2.3. Western blot analysis

RAW264.7 cells were cultured for 4 days just the same as the previously mentioned ones. Then the total proteins were collected for NFATc1 and c-fos immunoblotting. To detect the effect of PB on RANKL activated intracellular signal transduction cascades. Then the total proteins were collected after RANKL stimulation for 0, 5, 15 or 30 min. After that, each protein sample was subjected to SDS-PAGE and transferred to PVDF membranes. The membranes were blocked for 1 h, and incubated with rabbit anti-NFATc1, anti-c-fos, anti-phospho-NF-κB, anti-NF-κB, anti-phospho-ERK, anti-ERK, anti-phospho-p38, anti-p38, anti-phospho-JNK, and anti-JNK antibodies for 2 h. The membranes were then washed and incubated with horseradish peroxidase-conjugated goat anti-rabbit IgG for 1 h. After washed, the immunoreactive bands were visualized.

2.4. Real-time PCR analysis

RAW264.7 cells were cultured for 4 days with exactly the same procedure as before. Total RNA was isolated from osteoclast using a RNeasy Mini kit (Qiagen, Valencia, CA, USA), quantitative real-time PCR analysis was performed to test mRNA expression of CK, matrix metalloproteinase 9 (MMP-9), TRAP and C-C chemokine ligand 5 (CCL5) using the primer sequences shown in Table 1. All quantitative real-time PCRs were performed using Roche Light Cycler 480 Real-Time PCR system (Roche, Sussex, UK), and all samples were run in triplicate. Relative quantities of the tested genes were normalized to GAPDH mRNA. Meanwhile, total RNA was extracted from bone tissues. Quantitative real-time PCR analysis was performed to test mRNA expression of CCL5. Relative quantities of the tested genes were normalized to GAPDH mRNA.

2.5. Animals, protocols for drug administration

All animal experiments in this study were conducted according to the Guidelines for Animal Experimentation of Shandong University (Ethics number: GD201827). Twelve-week old male Wistar rats (Animal Center of Shandong University, Jinan, China) with an average body weight of 250 g were applied in this study. All rats were randomly distributed into 2 groups: the control group, where rats were received a phosphate buffered saline (PBS) for 6 weeks ($n = 10$); the PB group, where rats were orally administered PB (60 mg/kg/day) for 6 weeks ($n = 10$).

Table 1
Oligonucleotide primers used for real-time PCR.

Gene name		Oligonucleotide Sequence (5' → 3')
mouse-Cathepsin K	Forward	TGGTTCCTGTTGGGCTTTC
	Reverse	TCCGTTCTGCTGCAGGTATT
mouse-MMP-9	Forward	CGCTCATGTACCCGCTGTAT
	Reverse	CCGTGGGAGGTATAGTGGGA
mouse-TRAP	Forward	CTTTGTAGCCGTGGGTGACT
	Reverse	GGGAGCGGTGAGAGAATACG
mouse-GAPDH	Forward	TTGCAGTGGCAAAGTGGAGA
	Reverse	ACTGTGCCGTTGAATTTGCC
mouse-CCL5	Forward	GGTACCATGAAGATCTCTGCA
	Reverse	AGCAAGCCATGACAGGGAAGC

2.6. Serum biochemical analysis

Blood samples were collected before rats were sacrificed. Serum samples were separated by centrifuging at 2500 g for 10 min at 4 °C and stored at –80 °C. Serum markers for bone metabolism, including and tartrate-resistant acid phosphatase 5b (TRAP-5b) and bone specific alkaline phosphatase (BALP), were detected using enzyme-linked immunosorbent assay (ELISA) kit (Westang Biological Technology Co., Ltd., Shanghai, China) according to the protocols provided by manufacturers. Meanwhile, body weights were recorded after 6 weeks of drug administration.

2.7. Tissue processing

All the animals were anesthetized and fixed with 4% paraformaldehyde by transcardial perfusion. After that, tibiae were dissected and immersed in paraformaldehyde for additional 24 h. After that, bone tissues were decalcified with 10% EDTA-2Na for 4 weeks. Then the samples were dehydrated through an ascending ethanol series and embedded in paraffin. Serial longitudinal 5 μm thick sections were made for subsequent histological analysis.

2.8. Micro CT

Tibiae were scanned by Micro-CT (Inveon CT, Siemens, Germany) with a scanning resolution of 15 μm, a voltage of 80 kV and a current of 500 μA. Trabecular bone data were obtained at a region of interest, which is along the long axis of the proximal tibiae, and 1–3 mm away from the growth plate (Fig. 3E). VGStudio MAX (Volume Graphics, Germany) was used for 3D reconstructing image and data analysis. The bone histomorphometry parameters analysis included the cancellous portion of bone mineral density (BMD), bone mineral content (BMC), bone volume/total volume (BV/TV), trabecular thickness (Tb.Th), trabecular number (Tb.N) and trabecular separation (Tb.Sp). All evaluations were conducted in triplicate.

2.9. Histological detection

Hematoxylin and eosin (H&E) staining was applied to assess histological alterations. After being dewaxed and hydrated, the prepared sections were stained with Hematoxylin for 15 min and washed with distilled water. The sections were then immersed in Eosin for 10 min, washed again, dehydrated and mounted. Finally, the stained sections were observed and digital images were acquired.

2.10. TRAP staining and immunohistochemistry

Prepared sections were immersed in 0.3% hydrogen peroxide in PBS for 30 min and blocked with 1% bovine serum albumin (BSA; seologicals proteins Inc. Kankakee, IL, USA) in PBS (1% BSA-PBS) for 20 min. After that, the sections were incubated in the primary antibodies, at a dilution of 1:100 rabbit antibody against ALP, at a dilution of 1:100 rabbit antibody against OPN and at a dilution of 1:100 with 1% BSA-PBS for 2 h at room temperature, respectively. They were then washed and incubated in secondary antibodies of swine anti-rabbit at a dilution of 1:100 for 1 h at room temperature. Satisfactory immunostaining was acquired in the presence of diaminobenzidine (DAB) (Sigma-Aldrich, St. Louis, MO, USA). TRAP staining was proceeded like our previous study [23]. Finally, the staining results were observed and digital images were taken.

2.11. Image measurement and statistical analysis

Image Pro Plus 6.2 software was applied for assessing the trabecular area (Tb.Ar) and total bone area (T.Ar). Ratio of trabecular area (%Tb.Ar) was calculated by formula $Tb.Ar/T.Ar * 100\%$. Mean optical

density of images was analyzed manually using the software mentioned above. Positive reaction areas of ALP and OPN were selected by color cube-based manner. Meanwhile, multinucleated TRAP-positive cells were manually scored as osteoclasts. All values are presented as means ± standard (SD) deviation. The normality test of all data was performed. For data groups that conformed to the normal distribution, we performed Student's *t*-test to assess the differences between the two groups and performed one-way ANOVA to assess the differences among multiple groups. For data groups that did not conform to the normal distribution, we performed the rank sum test. $P < 0.05$ was considered statistically significant. Means with different letters (a, b, c and d) differ significantly from each other.

3. Results

3.1. PB down-regulates osteoclast differentiation and potential bone resorption

TRAP staining and pit formation assay were applied to detect osteoclast differentiation, formation and bone resorption ability. We first evaluated the direct effects of PB on RANKL-induced osteoclast formation. From the results of TRAP staining, decreasing number of osteoclast with TRAP-positive small cell bodies and few nuclei were notably identified in the PB group as compared with the control group (Fig. 1A). Next, to determine the effect of PB on osteoclastic activity, we employed pit formation assay. RAW264.7 cells were cultured under similar conditions. After that, the number and the area of resorption pits remarkably shrank in PB-treated group (Fig. 1B). From the results of histograms coverage rate, number and nuclei of TRAP-positive large cells were significantly decreased after PB stimulation. Same tendency of statistical differences can be seen in the bone resorption area rate (Fig. 1C). These results implied that PB negatively regulates RANKL-induced osteoclastic differentiation and function. Furthermore, this phenomenon of suppression becomes more and more obvious in the concentration of PB rising from 0 μM to 200 μM. Moreover, all of the four measured indexes previously mentioned get no significant change in the concentration range higher than 200 μM. Thus, we selected the PB concentration of 200 μM in following assays.

3.2. PB down-regulates osteoclast differentiation by NF-κB and MAPKs signaling pathways

Western blotting was applied to detect osteoclastic critical transcriptional factors and signaling pathways phosphorylation level. We next confirmed the regulation of PB on RANKL-induced osteoclast differentiation by analyzing the expression levels of osteoclastic critical transcriptional factors. Western blotting showed that expression levels of both NFATc1 and c-fos induced by RANKL were down-regulated in response to PB as compared with the control group (Fig. 2A). To gain insight into the mechanism of differential mediation of RANKL-induced osteoclastogenesis by PB, we performed immunoblot analysis of molecules known to be critically involved in RANKL signaling pathways, including NF-κB and MAPKs (ERK, p38, and JNK). We, therefore, examined whether NF-κB and MAPKs phosphorylation were altered by PB. When RAW264.7 cells were pretreated with PB, NF-κB and MAPKs phosphorylation induced by RANKL were strongly suppressed when compared with the control group (Fig. 2B). Conjointly, these results clearly demonstrated that PB acted on precursor cells to down-regulate RANKL-induced expression of osteoclast-specific transcription factors, leading to decrease the subsequent osteoclast differentiation. Meanwhile, this process is closely related to the NF-κB, ERK, p38, and JNK signaling pathways. Moreover, PB was unable to induce NF-κB phosphorylation in 293 T cells (Fig. 2E). That means the effect of PB on RANKL signaling pathway is specific to osteoclast precursor cells.

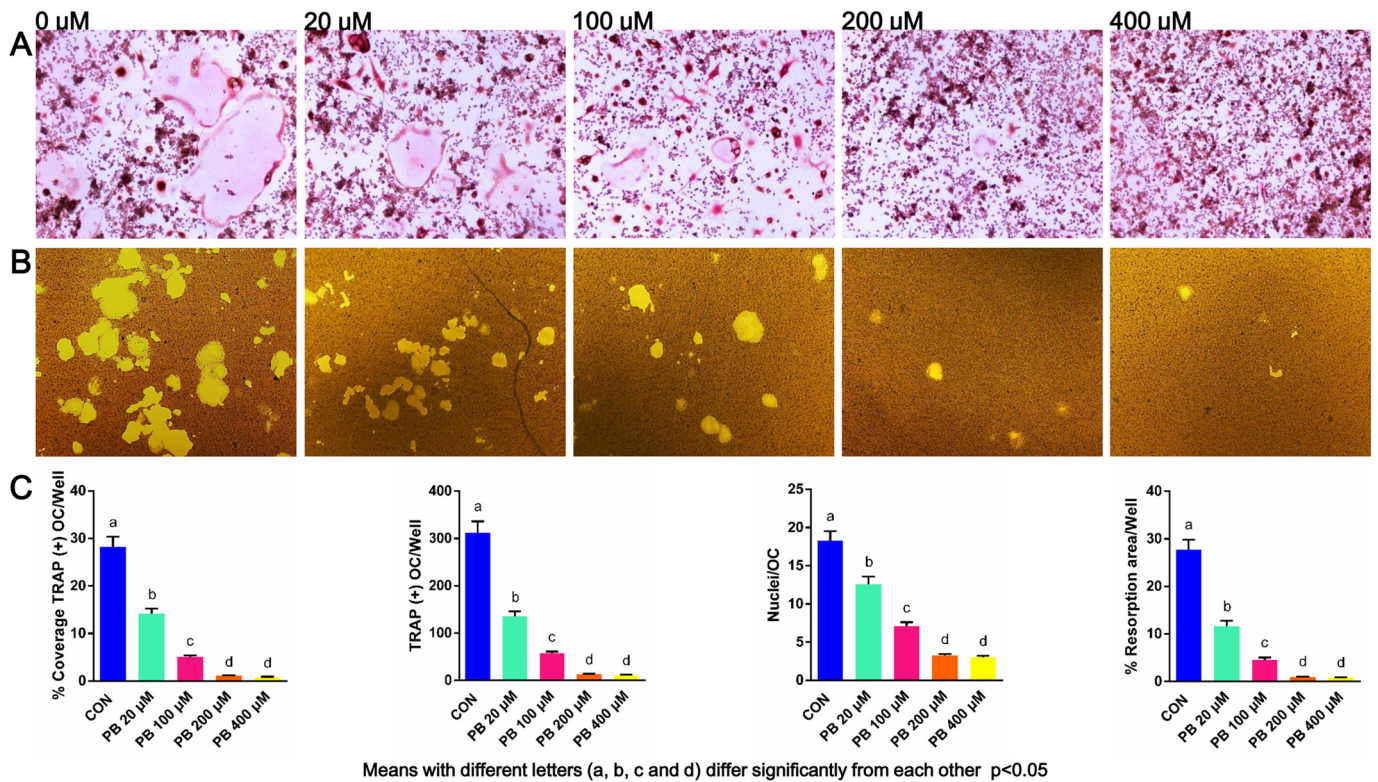


Fig. 1. The effect of PB on the down-regulation of osteoclast formation and bone resorption. RAW264.7 cells were cultured with RANKL-induced and in the presence of PB at 0 μM, 20 μM, 100 μM, 200 μM and 400 μM, respectively. After 7 days, TRAP staining was performed to visualize mature osteoclast followed by cell count, and the representative images were exhibited (A). Next, resorption pits were observed when RAW264.7 cells were cultured under similar conditions. After 10 days, cells were removed and the mineral-coated wells were counterstained by Von Kossa. Resorption pits were examined by light microscope, and the representative images were exhibited (B). The statistical differences of coverage rate, number and nuclei of TRAP-positive osteoclast and resorption area rate were presented in the histograms (C). All experiments were carried out at least three times. The data are expressed as mean ± SD. Different letters (a, b, c and d) indicate significant differences between groups ($p < 0.05$).

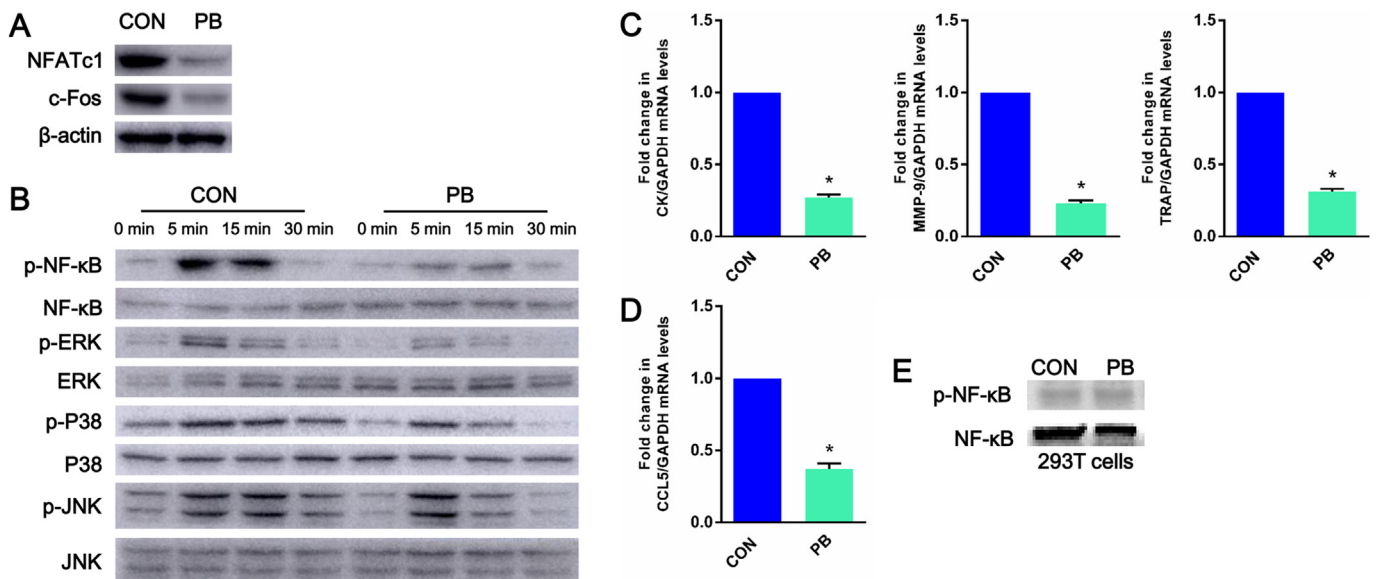


Fig. 2. The effect of PB on the down-regulation of osteoclast differentiation signaling pathways and osteoclast-specific genes. RAW264.7 cells were stimulated with PB and followed by RANKL treatment for 4 days. Cell lysates were collected and subjected to western blot analysis to determine the level of NFATc1 and c-fos expression (A). β-actin was served as a loading control (A). RAW264.7 cells were stimulated with PB and followed by RANKL treatment. Cell lysates were collected at the indicated time points and subjected to western blot analysis to determine the level of phosphorylation of indicated signaling molecules (B). Non phosphorylation groups were served as a loading control (B). RAW264.7 cells were stimulated with PB and followed by RANKL treatment for 4 days. After that, total RNA were extracted and subjected to quantitative real-time PCRs using probes specific for Cathepsin K, MMP-9, TRAP, CCL5 and GAPDH. The levels of genes mRNA expression were normalized to GAPDH expression (C and D). The data are representative of three independent experiments expressed as mean ± SD, (* $p < 0.05$). 293 T cells were stimulated with PB. Cell lysates were collected and subjected to western blot analysis to determine the level of phosphorylation of NF-κB (E). Non phosphorylation groups were served as a loading control (E).

3.3. PB down-regulates osteoclast-specific genes

Real-time PCR analysis was applied to detect the expression level of osteoclast-specific genes. We detected the regulation of PB on RANKL-induced osteoclast differentiation by analyzing the expression levels of osteoclastic critical marker genes. After that, the expression levels of CK, MMP-9 and TRAP mRNA induced by RANKL were decreased in response to PB as compared with the control group. Therefore, PB was responsible for the down-regulation of osteoclastic critical marker genes from the results of histograms (Fig. 2C). Moreover, we detected the regulation of PB on RANKL-induced osteoclast differentiation by analyzing the expression levels of CCL5 (the typical NF- κ B downstream target genes) gene. PB was responsible for the down-regulation of CCL5 gene from the results of histograms (Fig. 2D).

3.4. Histological analysis after 6 weeks of administration with PB

H&E staining and Micro-CT were applied to measure the bone histological parameters. After 6 weeks of AEDs administration, the PB group displayed a clear bone loss in histology compared to the control group, including decreased trabecular bone number, thinner metaphyseal trabeculae and increased trabecular spacing (Fig. 3A). Statistical analysis revealed several significant differences of %Tb.Ar from H&E staining between the two groups (Fig. 3B). Three-dimensional trabecular structure images obtained by Micro-CT also exhibited a same alteration for rats with AEDs administration (Fig. 3C). Comparing to the control group, the PB group observably decreased BMD, BMC, BV/TV, Tb.Th and Tb.N and significantly increased Tb.Sp (Fig. 3D). Statistical analysis revealed several significant differences between the two groups

Table 2

Data of histomorphometric parameters.

	Control	PB
Bone mineral density (BMD, mg/cm ³)	271 ± 12	235 ± 10*
Bone mineral content (BMC, mg)	1.07 ± 0.06	0.86 ± 0.06*
Bone volume/total volume (BV/TV, %)	48.2 ± 4.6	33.1 ± 2.2*
Trabecular thickness (Tb.Th, μ m)	90.1 ± 4.5	69.6 ± 4.7*
Trabecular number (Tb.N, 1/mm)	4.22 ± 0.14	2.76 ± 0.12*
Trabecular separation (Tb.Sp, μ m)	181 ± 13.8	274 ± 23.5*

* $p < 0.05$ vs. control.

with regard to the BMD, BMC, BV/TV, Tb.Th, Tb.N and Tb.Sp. All data were presented in Table 2.

3.5. Serum biochemical analysis after 6 weeks of administration with PB

Serum biochemical analysis was applied to measure the bone serum turnover makers. As shown in Fig. 4A and B, PB remarkably decreased bone resorption and bone formation serum makers TRAP-5b and BALP. Therefore, PB administration displayed a low bone turnover rate in rat models from the results of bone serum markers. Meanwhile, this suppression effect was more obvious in the side of bone formation than bone resorption. Besides, the PB group showed no differences in influencing on the body weight comparing to the control group (Fig. 4C).

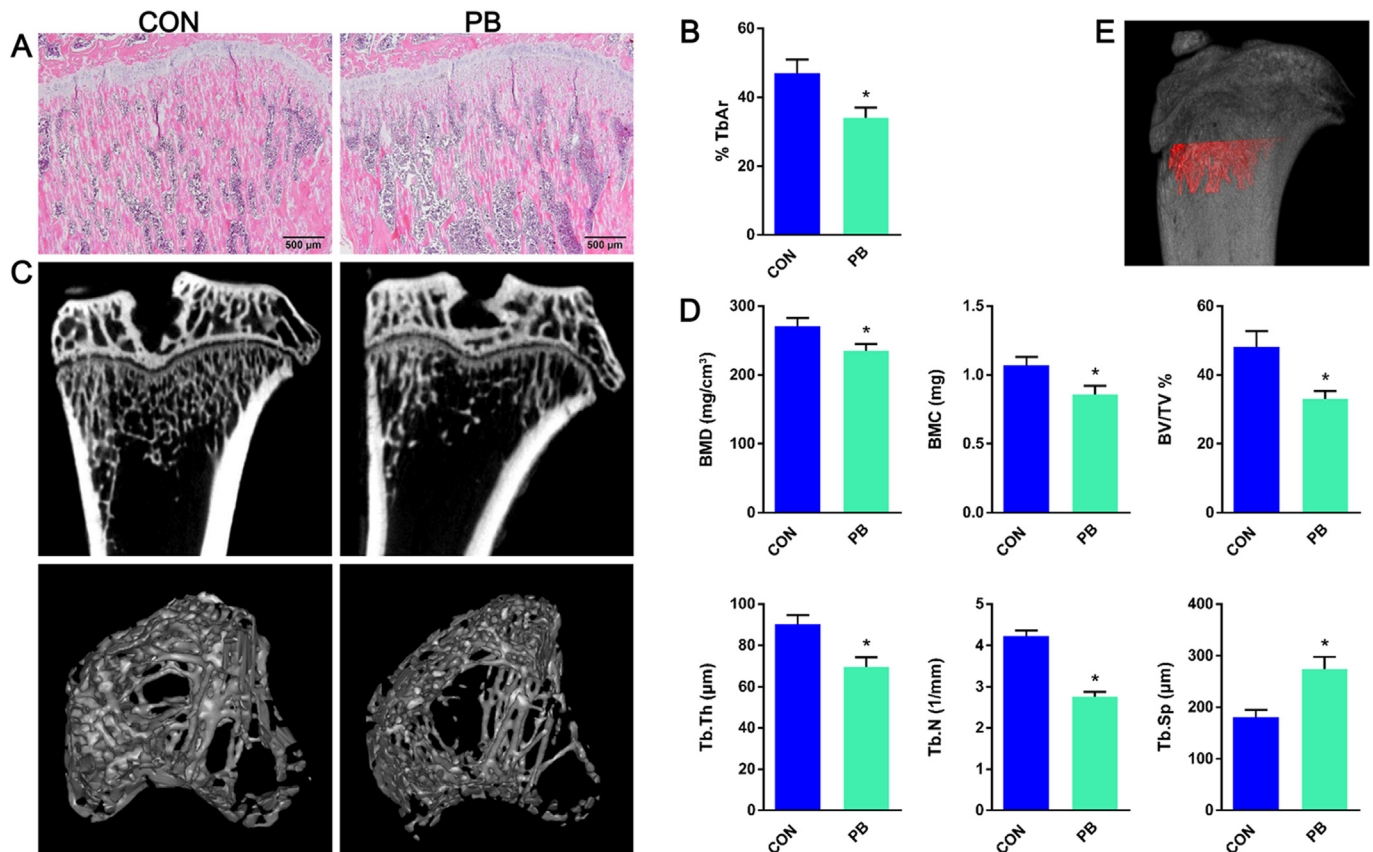


Fig. 3. Histological alterations revealed that PB administration increased bone loss.

Histological alterations from Hematoxylin and eosin (H&E) staining $\times 40$ (A). Changes of %Tb.Ar (B). Histological alterations from Micro-CT images (C). The first line is sagittal images of tibiae; the second line is coronal images of tibiae without cortical bone from the distal perspective. Changes of BMD, BMC, BV/TV, Tb.Th, Tb.N and Tb.Sp (D). Region of interest is along the long axis of the proximal tibiae, and 1–3 mm away from the growth plate (E). The data are representative of ten independent experiments expressed as mean \pm SD, (* $p < 0.05$).

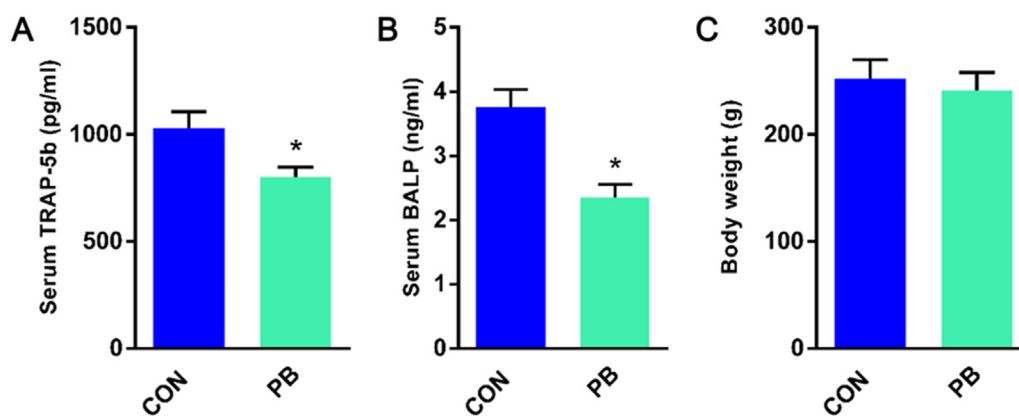


Fig. 4. Serum biochemical analysis revealed that PB administration decreased bone turnover markers. Histograms of serum TRAP-5b (A), serum BALP (B) and body weight (C). The data are representative of ten independent experiments expressed as mean \pm SD, (* $p < 0.05$).

Table 3

Data of serum indexes and body weight.

	Control	PB
Serum TRAP-5b (pg/ml)	1028 \pm 78	801 \pm 46*
Serum BALP (ng/ml)	3.76 \pm 0.27	2.35 \pm 0.21*
Body weight (g)	252 \pm 18	241 \pm 17*

* $p < 0.05$ vs. control.

All data were presented in Table 3.

3.6. TRAP staining and immunohistochemistry after 6 weeks of administration with PB

TRAP staining and immunohistochemistry were applied to evaluate the bone turnover condition. As expected, administration PB for 6 weeks considerably decreased the number of TRAP-positive osteoclasts as well as the immunoreactivity of ALP and OPN compared with the control group (Fig. 5A, B and C). Several significant differences between the two groups with regards to the number of TRAP positive osteoclasts and mean optical density of ALP and OPN are presented in the histograms (Fig. 5D). Therefore, PB administration exhibited a low bone turnover condition and a combined suppression effect on both bone resorption and bone formation on trabeculae bone surface. Notably, this suppression effect by PB was more obvious on bone formation than that on bone resorption. Moreover, after extracted total RNA from bone tissues in vivo, we detected the regulation of PB on osteoclast differentiation by analyzing the expression levels of CCL5 gene. PB was responsible for the down-regulation of CCL5 gene from the results of histograms (Fig. 5E).

4. Discussion

After PB stimulation, RANKL-induced osteoclast differentiation and function were gradually inhibited with the increasing of concentration. This effect was significantly observed in vitro when PB is up to 200 μ M. Next, our results showed that NF- κ B subunit p65 phosphorylation is strongly down-regulated by PB. That means PB decreases RANKL-induced osteoclastogenesis and potential bone resorption through NF- κ B signaling pathway. Specifically, NFATc1 and c-fos, two of the most crucial transcriptional factors for osteoclast differentiation displayed down-regulated tendency. It demonstrated that PB negatively regulates RANKL-induced osteoclastogenesis at transcriptional level. MAPKs (ERK, p38 and JNK) signaling pathways are known to be closely related to receptor activator of nuclear factor kappa-B (RANK) signaling transduction and are required for subsequent osteoclast formation

[24–27]. In this study, we have testified that PB clearly down-regulates ERK, p38 and JNK activation induced by RANKL, respectively. This may be due to the cross-talk between NF- κ B and MAPKs signaling pathways. Meanwhile, we can also draw a conclusion that CK, MMP-9, and TRAP, osteoclast-specific genes, are intensely suppressed by PB. This is another important evidence about PB influenced on osteoclast differentiation and function in vitro.

Bone turnover comprises two continuous processes: the removal of old bone (resorption by osteoclast) and the laying down of new bone (formation by osteoblast). ALP represents the osteoblast activity (markers of bone formation), while TRAP represents the osteoclast activity (markers of bone resorption). OPN regulates the formation and remodeling of mineralized tissue, and also provides as a coupling protein for osteoclastic resorption. Meanwhile, the balance between the osteoblast and osteoclast numbers, and their activities, determines the quality and quantity of bone [28]. Therefore, in order to test the pharmacological action on osteoclast in vivo, we investigated the treatment effect of PB (60 mg/kg/day) for 6 weeks in rats. From the result of histological analysis, tibiae displayed a clear feature of bone loss both in H&E staining and three-dimensional trabecular structure images. In immunohistochemistry, PB significantly decreased the number of osteoclast. Moreover, the suppression effect on osteoblast was more obvious than the same effect on osteoclast with a low level expression of ALP. Thus, the immunoreactivity of OPN were also reduced. Both two sides alteration are consistent with the change of bone serum markers such as TRAP-5b and BALP. That means PB can reduce bone turnover rate in vivo, and the process of bone loss can be realized through direct effects on osteoclast and osteoblast. Simultaneously, combined the results of immunohistochemistry and serum biochemical analysis, we considered that the bone loss after PB administration is due to the higher suppression effect on bone formation than that on bone resorption.

Several previous studies sustained our results. Kanda et al. reported that the administration of AEDs to rats significantly decrease bone strength and BMD, which is associated with enhanced bone resorption [29]. Tsukahara et al. proved that long-term antiepileptic treatment induce a state of decreased bone turnover in children, resulting in osteopenia preferentially in males [30]. Identically, in this study, oral administration of PB at a dose of 60 mg/kg/day for 6 weeks obviously induced the bone loss in rats. Besides, Yan et al. demonstrated that PB treatment inhibits chondrogenesis and proliferation of chondrocytes, and later it maybe influences ossification by inhibiting the proliferation of osteoblasts and vascular invasion [31]. Dent et al. reported that long-term anticonvulsant therapy such as PB can cause osteomalacia in patients [32]. Both of their articles are consistent with our vivo study. PB showed the same suppression effect on osteoblast. In addition, Hahn

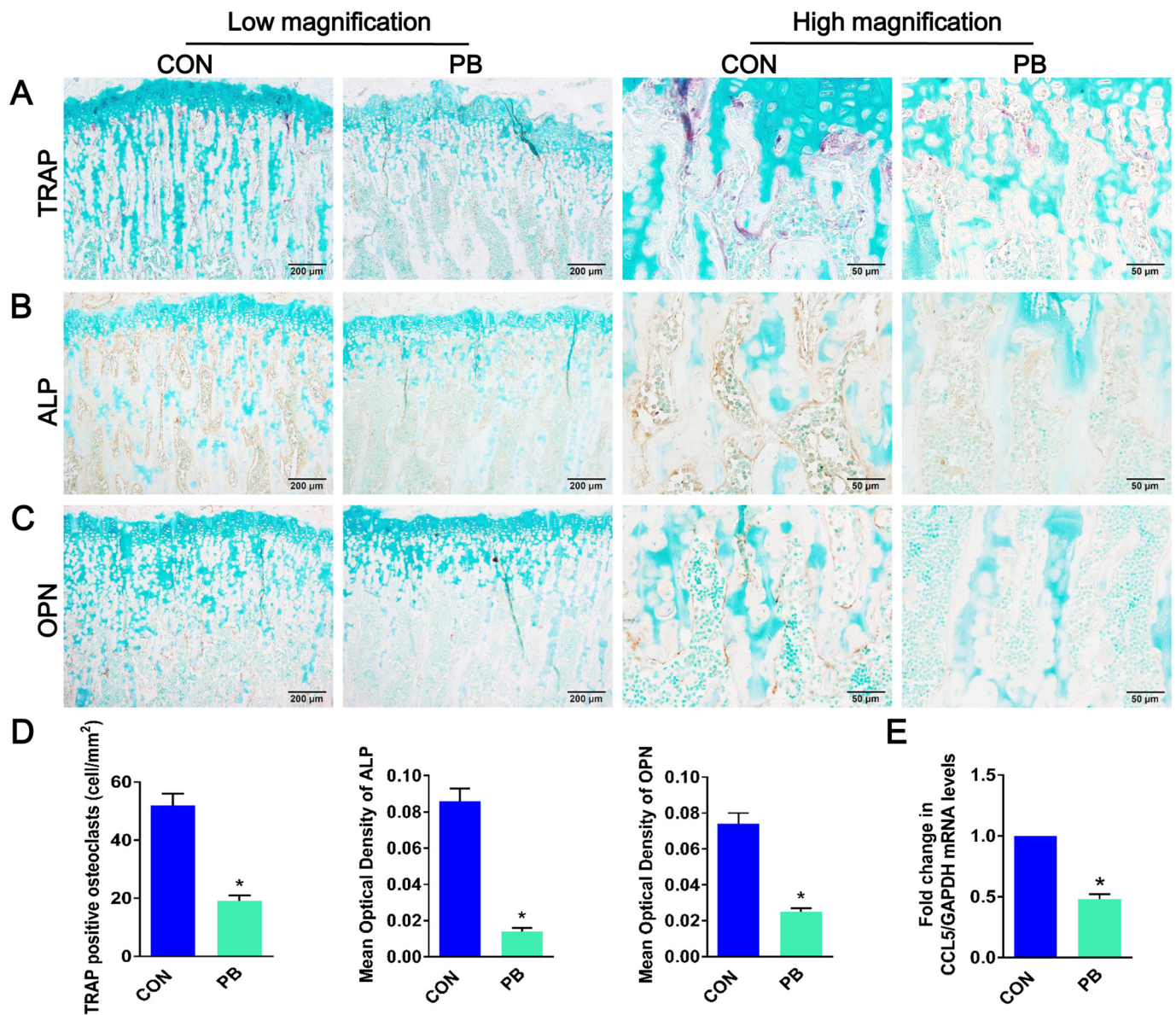


Fig. 5. TRAP staining and immunohistochemistry revealed that PB administration decreased bone turnover rate.

TRAP staining (A), immunohistochemistry of ALP (B) and OPN (C). TRAP positive cells (purple color), ALP positive cells (brown color) and OPN positive areas (brown color) were found on the surface of trabecular bone. Low magnification images were in the left two columns $\times 100$. High magnification images were in the right two columns $\times 400$. Changes of TRAP-positive osteoclasts, mean optical density of ALP and OPN (D). The data are representative of ten independent experiments expressed as mean \pm SD, ($*p < 0.05$). Total RNA were extracted from bone tissues and subjected to quantitative real-time PCRs using probes specific for CCL5 and GAPDH. The levels of CCL5 mRNA expression were normalized to GAPDH expression (E). The data are representative of three independent experiments expressed as mean \pm SD, ($*p < 0.05$). (For interpretation of the references to color in this figure legend, the reader is referred to the web version of this article.)

et al. reported that both phenytoin and PB can inhibit parathyroid hormone stimulated and 1,25 (OH)₂D stimulated bone resorption [33]. But this is an indirect function. Koide et al. demonstrated that phenytoin inhibits osteoclast differentiation and function through suppression of NFATc1 signaling [21]. In this study, we have testified for the first time that PB exhibit a direct suppression effect on osteoclast through decreasing phosphorylation level of NF- κ B and MAPKs signaling pathway in vitro.

Interestingly, AEDs most commonly associated with bone disorders are known to induce enzymes of the cytochrome P450 system [34,35]. CYP450-inducing AEDs, such as PB, upregulate the enzymes responsible for the metabolism of vitamin D, resulting in conversion of 25 (OH) vitamin D into inactive metabolites. The resulting decrease in 1,25 (OH)₂ vitamin D leads to reduced calcium absorption, with consecutive secondary hyperparathyroidism, increased bone resorption and

accelerated bone loss [20]. Specifically, there is decreased absorption of calcium from the gut that can be attributed to the decrease in biologically active forms of vitamin D resulting in hypocalcemia and feedback hypersecretion of circulating PTH. Hyperparathyroidism leads to increased bone resorption and ultimately reduced BMD and increased fracture risk [20,36]. Deficiency of Vitamin D which is essential for the bone growth and remodeling is commonly described as a cause for the bone loss in epileptic patients [37]. The Medicines and Healthcare products Regulatory Agency recommends considering prophylactic Vitamin D supplementation for patients at risk treated with liver enzyme-inducing AEDs. That's why vitamin D supplementation can reduce fracture and bone loss. This is an indirect mechanism of bone loss induced by PB. Other mechanisms include direct inhibition effects of AEDs on calcitonin secretion [20,38]. Meanwhile, since angiogenesis plays a crucial role during bone ossification and formation. Some

researchers reported that PB can directly inhibit osteoblast by influence on vascular invasion and chondrocytes development [31]. But we applied immunohistochemistry on bone tissue to observe the direct suppression effect of PB on osteoclast and osteoblast in this study. Meanwhile, these results were identical with serum biochemical analysis and osteoclast culture in vitro. We considered that this direct suppression effect on bone cells play a pivotal role during the process of AEDs induced bone loss. It will benefit in-depth research of the relationship between AEDs and bone metabolism.

5. Conclusion

Taken together, we have testified for the first time that RANKL-induced osteoclast differentiation and function were significantly inhibited in vitro when PB is up to 200 μ M. This direct suppression effect on osteoclast is performed through decreasing phosphorylation level of NF- κ B and MAPKs signaling pathway. Meanwhile, oral administration of PB at a dose of 60 mg/kg/day for 6 weeks obviously induced the bone loss in rats. Moreover, this bone loss is due to the higher suppression effect by PB on osteoblast-induced bone formation than that on osteoclast-induced bone resorption.

Acknowledgements

We thank all the subjects who participated in this study. This work was supported by Shandong Provincial Natural Science Foundation (No. ZR2016CQ18), the China Postdoctoral Science Foundation funded project (Nos. 2015M580592, 2016T90637) to Zheng X, and the National Natural Science Foundation of China (Nos. 81470719, 81611140133) to Li M.

Conflict of interest

The authors declare that they have no conflict of interest.

References

- [1] S.L. Teitelbaum, F.P. Ross, Genetic regulation of osteoclast development and function, *Nat. Rev. Genet.* 4 (8) (2003) 638–649.
- [2] H. Yoshida, S. Hayashi, T. Kunisada, M. Ogawa, S. Nishikawa, H. Okamura, T. Sudo, L.D. Shultz, S. Nishikawa, The murine mutation osteopetrosis is in the coding region of the macrophage colony stimulating factor gene, *Nature* 345 (6274) (1990) 442–444.
- [3] W.J. Boyle, W.S. Simonet, D.L. Lacey, Osteoclast differentiation and activation, *Nature* 423 (6937) (2003) 337–342.
- [4] L.C. Hofbauer, S. Khosla, C.R. Dunstan, D.L. Lacey, W.J. Boyle, B.L. Riggs, The roles of osteoprotegerin and osteoprotegerin ligand in the paracrine regulation of bone resorption, *J. Bone Miner. Res.* 15 (1) (2000) 2–12.
- [5] T. Suda, N. Takahashi, N. Udagawa, E. Jimi, M.T. Gillespie, T.J. Martin, Modulation of osteoclast differentiation and function by the new members of the tumor necrosis factor receptor and ligand families, *Endocr. Rev.* 20 (3) (1999) 345–357.
- [6] H. Takayanagi, S. Kim, T. Koga, H. Nishina, M. Isshiki, H. Yoshida, A. Saiura, M. Isobe, T. Yokochi, J. Inoue, E.F. Wagner, T.W. Mak, T. Kodama, T. Taniguchi, Induction and activation of the transcription factor NFATc1 (NFAT2) integrate RANKL signaling in terminal differentiation of osteoclasts, *Dev. Cell* 3 (6) (2002) 889–901.
- [7] M. Asagiri, K. Sato, T. Usami, S. Ochi, H. Nishina, H. Yoshida, I. Morita, E.F. Wagner, T.W. Mak, E. Serfling, H. Takayanagi, Autoamplification of NFATc1 expression determines its essential role in bone homeostasis, *J. Exp. Med.* 202 (9) (2005) 1261–1269.
- [8] T.J. Chambers, C.J. Magnis, Calcitonin alters behaviour of isolated osteoclasts, *J. Pathol.* 136 (1) (1982) 27–39.
- [9] H.K. Vaananen, H. Zhao, M. Mulari, J.M. Halleen, The cell biology of osteoclast function, *J. Cell Sci.* 113 (Pt 3) (2000) 377–381.
- [10] H. Zhao, H.K. Vaananen, Pharmacological sequestration of intracellular cholesterol in late endosomes disrupts ruffled border formation in osteoclasts, *J. Bone Miner. Res.* 21 (3) (2006) 456–465.
- [11] I. Nakamura, N. Takahashi, T. Sasaki, S. Tanaka, N. Udagawa, H. Murakami, K. Kimura, Y. Kabuyama, T. Kurokawa, T. Suda, et al., Wortmannin, a specific inhibitor of phosphatidylinositol-3 kinase, blocks osteoclastic bone resorption, *FEBS Lett.* 361 (1) (1995) 79–84.
- [12] H. Suzuki, I. Nakamura, N. Takahashi, T. Ikuhara, K. Matsuzaki, Y. Isogai, M. Hori, T. Suda, Calcitonin-induced changes in the cytoskeleton are mediated by a signal pathway associated with protein kinase A in osteoclasts, *Endocrinology* 137 (11) (1996) 4685–4690.
- [13] J. Engel Jr., Etiology as a risk factor for medically refractory epilepsy: a case for early surgical intervention, *Neurology* 51 (5) (1998) 1243–1244.
- [14] H.C. Fan, H.S. Lee, K.P. Chang, Y.Y. Lee, H.C. Lai, P.L. Hung, H.F. Lee, C.S. Chi, The impact of anti-epileptic drugs on growth and bone metabolism, *Int. J. Mol. Sci.* 17 (8) (2016).
- [15] S.A. Lowe, Drugs in pregnancy. Anticonvulsants and drugs for neurological disease, *Best Pract. Res. Clin. Obstet. Gynaecol.* 15 (6) (2001) 863–876.
- [16] B.J. Wlodarczyk, A.M. Palacios, T.M. George, R.H. Finnell, Antiepileptic drugs and pregnancy outcomes, *Am. J. Med. Genet. Part A* 158A (8) (2012) 2071–2090.
- [17] J.M. Nicholas, L. Ridsdale, M.P. Richardson, M. Ashworth, M.C. Gulliford, Trends in antiepileptic drug utilisation in UK primary care 1993–2008: cohort study using the general practice research database, *Seizure* 21 (6) (2012) 466–470.
- [18] T.J. Hahn, S.J. Birge, C.R. Scharp, L.V. Avioli, Phenobarbital-induced alterations in vitamin D metabolism, *J. Clin. Invest.* 51 (4) (1972) 741–748.
- [19] N. Jette, L.M. Lix, C.J. Metge, H.J. Prior, J. McChesney, W.D. Leslie, association of antiepileptic drugs with nontraumatic fractures: a population-based analysis, *Arch. Neurol.* 68 (1) (2011) 107–112.
- [20] L.A. Fitzpatrick, Pathophysiology of bone loss in patients receiving anticonvulsant therapy, *Epilepsy Behav.* 5 (Suppl. 2) (2004) S3–15.
- [21] M. Koide, S. Kinugawa, T. Ninomiya, T. Mizoguchi, T. Yamashita, K. Maeda, H. Yasuda, Y. Kobayashi, H. Nakamura, N. Takahashi, N. Udagawa, Diphenylhydantoin inhibits osteoclast differentiation and function through suppression of NFATc1 signaling, *J. Bone Miner. Res.* 24 (8) (2009) 1469–1480.
- [22] K. Oda, Y. Amaya, M. Fukushi-Irie, Y. Kinameri, K. Ohsuye, I. Kubota, S. Fujimura, J. Kobayashi, A general method for rapid purification of soluble versions of glycosylphosphatidylinositol-anchored proteins expressed in insect cells: an application for human tissue-nonspecific alkaline phosphatase, *J. Biochem.* 126 (4) (1999) 694–699.
- [23] M. Li, T. Hasegawa, H. Hogo, S. Tatsumi, Z. Liu, Y. Guo, M. Sasaki, C. Tabata, T. Yamamoto, K. Ikeda, N. Amizuka, Histological examination on osteoblastic activities in the alveolar bone of transgenic mice with induced ablation of osteocytes, *Histol. Histopathol.* 28 (3) (2013) 327–335.
- [24] E. Ang, Q. Liu, M. Qi, H.G. Liu, X. Yang, H. Chen, M.H. Zheng, J. Xu, Mangiferin attenuates osteoclastogenesis, bone resorption, and RANKL-induced activation of NF- κ B and ERK, *J. Cell. Biochem.* 112 (1) (2011) 89–97.
- [25] H. Tao, M. Okamoto, M. Nishikawa, H. Yoshikawa, A. Myoui, P38 mitogen-activated protein kinase inhibitor, FR167653, inhibits parathyroid hormone related protein-induced osteoclastogenesis and bone resorption, *PLoS One* 6 (8) (2011) e23199.
- [26] F. Ikeda, T. Matsubara, T. Tsurukai, K. Hata, R. Nishimura, T. Yoneda, JNK/c-Jun signaling mediates an anti-apoptotic effect of RANKL in osteoclasts, *J. Bone Miner. Res.* 23 (6) (2008) 907–914.
- [27] B.R. Wong, D. Besser, N. Kim, J.R. Arron, M. Vologodskaja, H. Hanafusa, Y. Choi, TRANCE, a TNF family member, activates Akt/PKB through a signaling complex involving TRAF6 and c-Src, *Mol. Cell* 4 (6) (1999) 1041–1049.
- [28] A.B. Khalid, S.A. Krum, Estrogen receptors alpha and beta in bone, *Bone* 87 (2016) 130–135.
- [29] J. Kanda, N. Izumo, Y. Kobayashi, K. Onodera, T. Shimakura, N. Yamamoto, H.E. Takahashi, H. Wakabayashi, Effects of the antiepileptic drugs phenytoin, gabapentin, and Levetiracetam on bone strength, bone mass, and bone turnover in rats, *Biol. Pharm. Bull.* 40 (11) (2017) 1934–1940.
- [30] H. Tsukahara, K. Kimura, Y. Todoroki, Y. Ohshima, M. Hiraoka, Y. Shigematsu, Y. Tsukahara, M. Miura, M. Mayumi, Bone mineral status in ambulatory pediatric patients on long-term anti-epileptic drug therapy, *Pediatr. Int.* 44 (3) (2002) 247–253.
- [31] Y. Yan, X. Cheng, R.H. Yang, H. Li, J.L. Chen, Z.L. Ma, G. Wang, M. Chuai, X. Yang, Exposure to excess phenobarbital negatively influences the osteogenesis of Chick embryos, *Front. Pharmacol.* 7 (2016) 349.
- [32] C.E. Dent, A. Richens, D.J. Rowe, T.C. Stamp, Osteomalacia with long-term anticonvulsant therapy in epilepsy, *Br. Med. J.* 4 (5727) (1970) 69–72.
- [33] T.J. Hahn, C.R. Scharp, C.A. Richardson, L.R. Halstead, A.J. Kahn, S.L. Teitelbaum, Interaction of diphenylhydantoin (phenytoin) and phenobarbital with hormonal mediation of fetal rat bone resorption in vitro, *J. Clin. Invest.* 62 (2) (1978) 406–414.
- [34] J.M. Nicholas, L. Ridsdale, M.P. Richardson, A.P. Grieve, M.C. Gulliford, Fracture risk with use of liver enzyme inducing antiepileptic drugs in people with active epilepsy: cohort study using the general practice research database, *Seizure* 22 (1) (2013) 37–42.
- [35] A. Verrotti, R. Greco, G. Morgese, F. Chiarelli, Increased bone turnover in epileptic patients treated with carbamazepine, *Ann. Neurol.* 47 (3) (2000) 385–388.
- [36] J. Feldkamp, A. Becker, O.W. Witte, D. Scharf, W.A. Scherbaum, Long-term anticonvulsant therapy leads to low bone mineral density—evidence for direct drug effects of phenytoin and carbamazepine on human osteoblast-like cells, *Exp. Clin. Endocr. Diab.* 108 (1) (2000) 37–43.
- [37] D.L. Andress, J. Ozuna, D. Tirschwell, L. Grande, M. Johnson, A.F. Jacobson, W. Spain, Antiepileptic drug-induced bone loss in young male patients who have seizures, *Arch. Neurol.* 59 (5) (2002) 781–786.
- [38] R.H. Lee, K.W. Lyles, C. Colon-Emeric, A review of the effect of anticonvulsant medications on bone mineral density and fracture risk, *Am. J. Geriatr. Pharmacother.* 8 (1) (2010) 34–46.